Chapter 6

Nucleon Structure and the Parton Model

1. Electron-Proton Elastic Scattering

Electron scattering provides the most powerful tool for revealing the internal structure of the nucleon. Much of the theoretical background for understanding the formulations in electron scattering has already been discussed in the last chapter. We begin by summarizing the relevant cross sections corresponding to different assumptions used in treating the e^--p scattering.

1) Spin-0 Particle Scattering off a Static Point Spin-0 Particle with Charge e

Recall Equation 5.45

$$\left(\frac{d\sigma}{d\Omega}\right)_{cm} = \frac{\alpha^2}{4s}\frac{P_f}{P_i}\frac{(s-u)^2}{t^2} \tag{6.1}$$

for scattering of spin-0 particle off a spin-0 particle. A static target is represented by $M >> m$, where m, M are the incident and target mass respectively.

$$P_a = \left(E_a, \vec{K}\right)$$

$$P_b = (M, 0) = P_b'$$

$$P_a' = \left(E_a', \vec{K}'\right)$$

$$s = \left(P_a + P_b\right)^2 = P_a^2 + 2E_a M + M^2$$

$$u = \left(P_a - P_b'\right)^2 = P_a^2 - 2E_a' M + M^2$$

For $M \gg m,\ |K| \simeq |K'|,\ E_a \simeq |K|,\ E_a' \simeq |K'|,\ E_a \simeq E_a'$

$$s-u \simeq 4E_a M \simeq 4|K|M$$

$$t \simeq -4|K|^2 \sin^2\frac{\theta}{2}$$

$$s \simeq M^2$$

$$P_f \simeq P_i$$

Hence Equation 6.1 becomes

$$\left(\frac{d\sigma}{d\Omega}\right)_{cm} \simeq \frac{\alpha^2}{4M^2}\frac{\left(4|K|M\right)^2}{\left(4|K|^2 \sin^2\theta/2\right)^2} = \frac{\alpha^2}{4|K|^2 \sin^4\theta/2} \tag{6.2}$$

which is recognized as the Rutherford scattering.

2) Spin-½ Electron Scattering off a Static Spin-0 Point-Charge *e*

We have already derived the cross section for this case. The expression is given in Equation 5.79. Namely,

$$\frac{d\sigma}{d\Omega} = \frac{\alpha^2 E^2}{4|K|^4 \sin^4\theta/2}\left(1 - v^2 \sin\frac{\theta}{2}\right) \tag{6.3}$$

This is the Mott scattering. Note that at high energy $v \to 1$, and the Mott scattering becomes

$$\frac{d\sigma}{d\Omega} = \frac{\alpha^2 E^2}{4|K|^4 \sin^4\theta/2}\cos^2\frac{\theta}{2} \tag{6.4}$$

and scattering to 180^o is forbidden. This can be understood by noting that helicity of the electron is conserved at high energy. The following illustration

shows that for electron scattered to 180°, the spin has to be flipped to conserve helicity. Since a spin-0 target cannot flip the electron spin, such scattering is forbidden.

3) Spin-½ Electron Scattering off a Spin-0 Static Composite Particle

The cross section in this case is worked out in Halzen and Martin, Ex. 8.1. The result is

$$\left(\frac{d\sigma}{d\Omega}\right)=\left(\frac{d\sigma}{d\Omega}\right)_{Mott}\left|F\left(\vec{q}\right)\right|^2 \tag{6.5}$$

where $F\left(\vec{q}\right)$ is the Fourier transform of the charge distribution $\rho(x)$:

$$F\left(\vec{q}\right)=\int d^3x\rho\left(x\right)\,e^{i\vec{q}\cdot\vec{x}} \tag{6.6}$$

4) Spin-½ Electron Scattering off a Spin-0 Point-like Particle which can Recoil

This case can be worked out by replacing the $L_{\mu\nu}^{muon}$ which spears in the $e^-\mu^-\rightarrow e^-\mu^-$ scattering by the $\left(p+p'\right)_\mu\left(p+p'\right)_\nu$ corresponding to the spin-0 vertex. The result, as shown in Ex. 6.8 of Halzen and Martin, is

$$\left(\frac{d\sigma}{d\Omega}\right)=\left(\frac{\alpha^2}{4E^2\sin^4\theta/2}\right)\frac{E'}{E}\cos^2\frac{\theta}{2} \tag{6.7}$$

where one assumes the electron mass is negligible. A comparison of Equations 6.7 and 6.4 shows that the recoil effect introduces the factor E'/E.

5) Spin-½ Electron Scattering off a Spin-½ Point Particle which can Recoil

This simply corresponds to $e^-\mu^-\rightarrow e^-\mu^-$ scattering which we worked out in Chapter 5. Recall Equation 5.82

$$\left(\frac{d\sigma}{d\Omega}\right)=\left(\frac{\alpha^2}{4E^2\sin^4\theta/2}\right)\left(\frac{E'}{E}\right)\left(\cos^2\frac{\theta}{2}-\frac{q^2}{2M^2}\sin^2\frac{\theta}{2}\right) \tag{6.8}$$

A comparison of Equations 6.8 and 6.7 shows that the spin-½ target leads to an additional term, $\frac{-q^2}{2M^2}\sin^2\frac{\theta}{2}$, which represents a magnetic interaction. The spin of the electron can therefore be flipped via the magnetic interaction. Equation 6.8 shows that electron can now scatter to 180°.

We are now ready to consider *ep* elastic scattering. The proton is no longer considered as a structureless point particle. Instead, proton is a spin-½ composite particle. The *ep* elastic scattering can be represented by the following diagram:

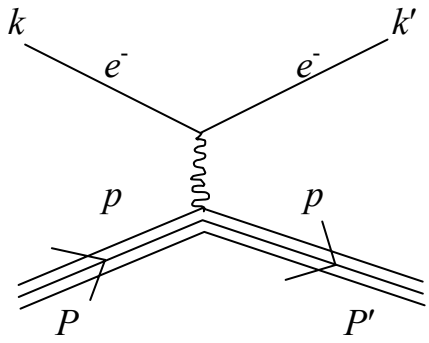

The transition matrix T_{fi} can be written as (Equation 5.17)

$$T_{fi}=-i\int j_\mu\left(-\frac{1}{q^2}\right)J^\mu d^4x \tag{6.9}$$

The current from the point-like electron is

$$j_\mu=-e\bar{u}\left(K'\right)\gamma_\mu u\left(K\right)e^{i(K'-K)\cdot x} \tag{6.10}$$

For the proton, the current can be written analogously as

$$J^\mu=e\bar{u}\left(p'\right)[\qquad]u\left(p\right)e^{i(p'-p)\cdot x} \tag{6.11}$$

Equation 6.11 reflects the fact that initial and final states of the hadron are protons (elastic scattering). However, the 4-vector represented by [ ] is no longer γ^μ.

One can write down a most general expression for the 4-vector, constructed out of the γ-matrices and the 4-momenta, p and p', as

$$\begin{aligned}[\qquad] &= K_1\gamma^\mu + K_2 i\sigma^{\mu\nu}\left(p'-p\right)_\nu + K_3 i\sigma^{\mu\nu}\left(p'+p\right)_\nu \\ &\quad + K_4\left(p'-p\right)^\mu + K_5\left(p'+p\right)^\mu\end{aligned} \tag{6.12}$$

Now, the "Gordon decomposition" can be used to express $\left(p'+p\right)^\mu$ in terms of γ^μ and $\sigma^{\mu\nu}\left(p'-p\right)_\nu$:

$$\bar{u}\left(p'\right)\gamma^\mu u\left(p\right) = \frac{1}{2m}\bar{u}\left(p'\right)\left[\left(p'+p\right)^\mu + i\sigma^{\mu\nu}\left(p'-p\right)_\nu\right]u\left(p\right) \tag{6.13}$$

Using Equation 6.13, the K_5 term can be expressed in terms of the K_1 and K_2 terms. Furthermore, it can be shown that

$$i\,\bar{u}\left(p'\right)i\sigma^{\mu\nu}\left(p'+p\right)_\nu u\left(p\right) = -\bar{u}\left(p'\right)\left(p'-p\right)^\mu u\left(p\right) \tag{6.14}$$

using the fact that $\left(\not{p}-m\right)u\left(p\right)=0$ and $\bar{u}\left(p'\right)\left(\not{p}'-m\right)=0$. Therefore, the K_3 term can be expressed in terms of the K_4 term. The $p'+p$ terms in Equation 6.12 are not independent of the other three terms.

A general expression for the hadronic current for proton in the *ep* scattering is

$$J^\mu = e\bar{u}\left(p'\right)\left[F_1\left(q^2\right)\gamma^\mu + \frac{\kappa}{2M}F_2\left(q^2\right)i\gamma^{\mu\nu}q_\nu + F_3\left(q^2\right)q^\mu\right]u\left(p\right)e^{i\left(p'-p\right)\cdot x} \tag{6.15}$$

Current conservation, $\partial_\mu J^\mu = 0$, implies that $q_\mu J^\mu = 0$ and we have

$$\begin{aligned}&F_1\left(q^2\right)\bar{u}\left(p'\right)\left(p'-p\right)u\left(p\right) + F_2\left(q^2\right)\bar{u}\left(p'\right)\frac{\kappa}{2m}q_\mu\sigma^{\mu\nu}q_\nu u\left(p\right) \\ &+F_3\left(q^2\right)\bar{u}\left(p'\right)q^2 u\left(p\right) = 0\end{aligned} \tag{6.16}$$

The first term in Equation 6.16 vanishes since $u\left(p\right)$, $\bar{u}\left(p'\right)$ satisfy the Dirac Equation. The second term is also equal to zero since $\sigma^{\mu\nu}$ is antisymmetric with

respect to $\mu\nu$ exchange. Therefore, $F_3\,(q^2) = 0$, and the hadronic current can be written as

$$J^\mu = e\bar{u}(p')\left[F_1(q^2)\gamma^\mu + \frac{\kappa}{2M}F_2(q^2)i\sigma^{\mu\nu}q_\nu\right]u(p)e^{i(p'-p)\bullet x} \qquad (6.17)$$

Equation 6.17 can be re-expressed - using the Gordon decomposition (Equation 6.13) – as

$$J^\mu = e\bar{u}(p')\left[\left[F_1(q^2)+\kappa F_2(q^2)\right]\gamma^\mu - \frac{\kappa F_2(q^2)}{2M}(p'+p)^\mu\right]u(p)e^{iq} \qquad (6.18)$$

For a point-like proton, $\kappa = 0$ and $F_1\,(q^2) = 1$. κ is the anomalous magnetic moment produced by the motion of the constituents. Note that F_1, F_2 are functions of q^2 only. Other Lorentz scalars, such as $p\bullet q$, can be expressed in terms of q^2.

To evaluate the *ep* elastic scattering cross section, we have

$$\overline{|M|^2} = \frac{e^4}{q^4}L_{\mu\nu}w^{\mu\nu}$$

where

$$w^{\mu\nu} = \frac{1}{2}\sum_{spin}\bar{u}\left[(F_1+\kappa F_2)\gamma^\mu - \frac{\kappa F_2}{2M}(p'+p)^\mu\right]u \left[\bar{u}\left[(F_1+\kappa F_2)\gamma^\nu - \frac{\kappa F_2}{2M}(p'+p)^\nu\right]u\right]^* \qquad (6.19)$$

and $L_{\mu\nu}$ is the leptonic tensor for the electrons (Equation 5.73).

Using standard techniques for calculating the traces, the three terms in $w^{\mu\nu}$ are:

1) $$\begin{aligned}&(F_1+\kappa F_2)^2\,tr\left[\left(\not{p}'+M\right)\gamma^\mu\left(\not{p}+M\right)\gamma^\nu\right]\\ &=4(F_1+\kappa F_2)^2\left[p'^\mu p^\nu + p'^\nu p^\mu - g^{\mu\nu}(p\bullet p') + g^{\mu\nu}M^2\right]\end{aligned}$$

2) $$\begin{aligned}&\frac{-\kappa F_2}{2M}(F_1+\kappa F_2)\,tr\left[\left(\not{p}'+M\right)\gamma^\mu\left(\not{p}+M\right)(p+p')^\nu\right]\\ &=-2\kappa F_2(F_1+\kappa F_2)^2(p+p')^\mu(p+p')^\nu\end{aligned}$$

3) $$\frac{-\kappa^2 F_2^2}{4M^2} tr\left[\left(\not{p}' + M\right)\left(p + p'\right)^\mu \left(\not{p} + M\right)\left(p + p'\right)^\nu\right]$$
$$= \frac{-\kappa^2 F_2^2}{4M^2}\left(p + p'\right)^2 \left(p + p'\right)^\mu \left(p + p'\right)^\nu$$

The *ep* elastic scattering cross section becomes

$$\left(\frac{d\sigma}{d\Omega}\right)_{lab} = \left(\frac{\alpha^2}{4E^2 \sin^4 \theta/2}\right)\frac{E'}{E}\left\{\left(F_1^2 - \frac{\kappa^2 q^2}{4M^2} F_2^2\right)\cos^2\frac{\theta}{2} - \frac{q^2}{2M^2}\left(F_1 + \kappa F_2\right)^2 \sin^2\frac{\theta}{2}\right\} \tag{6.20}$$

It is conventional to introduce the 'Sachs' form factors G_E and G_M:

$$\begin{aligned} G_E &= F_1 + \frac{\kappa q^2}{4M^2} F_2 \quad \left(\text{electric form factor}\right) \\ G_M &= F_1 + \kappa F_2 \qquad \left(\text{magnetic form factor}\right) \end{aligned} \tag{6.21}$$

and the *ep* elastic cross section is written as

$$\left(\frac{d\sigma}{d\Omega}\right)_{lab} = \left(\frac{\alpha^2}{4E^2 \sin^4 \theta/2}\right)\frac{E'}{E}\left(\frac{G_E^2 + \tau G_M^2}{1+\tau}\cos^2\frac{\theta}{2} + 2\tau G_M^2 \sin^2\frac{\theta}{2}\right) \tag{6.22}$$

where $\tau = -q^2/4M^2$.

For $q^2 \to 0$, the electron beam effectively sees a proton with charge e and magnetic moment of $\left(1+\kappa\right)e/2M$. We therefore have, from Equation 6.17,

$$F_1^P\left(0\right) = 1 \qquad F_2^P\left(0\right) = 1 \tag{6.23}$$

Similarly, for electron scattering off a neutron,

$$F_1^n(0)=0 \qquad F_2^n(0)=1 \tag{6.24}$$

Equation 6.21 gives

$$\begin{aligned} G_E^P(0)&=1 \qquad & G_E^n(0)&=0 \\ G_M^P(0)&=1+\kappa_p=\mu_p=2.79 \\ G_M^n(0)&=\kappa_n=\mu_n=-1.91 \end{aligned} \tag{6.25}$$

This shows that

$$G_E^P(0)=G_M^P(0)\Big/\mu_p \tag{6.26}$$

It is found experimentally that $G_E^P\left(Q^2\right)$ and $G_M^P\left(Q^2\right)$ have very similar Q^2 dependence, and

$$G_E^P\left(Q^2\right)\simeq G_M^P\left(Q^2\right)\Big/\mu_p \simeq \left(1+\frac{Q^2}{0.71\ \text{GeV}^2}\right)^{-2} \tag{6.27}$$

Recent data from Jefferson Lab showed, however, that $\mu_p G_E^P\left(Q^2\right)\Big/G_M^P\left(Q^2\right)$ starts to deviate from unity as Q^2 becomes large. The root-mean-square radius of the proton is determined to be

$$\begin{aligned} \left\langle r^2\right\rangle &= -6\frac{dG\left(Q^2\right)}{dQ^2}\bigg|_{Q^2\to 0} = 0.66\ \text{fm}^2 \\ \left\langle r^2\right\rangle^{1/2} &= 0.81\ \text{fm} \end{aligned} \tag{6.28}$$

2. Electron-Proton Inelastic Scattering

For an electron-proton inelastic scattering, ep → e′x,

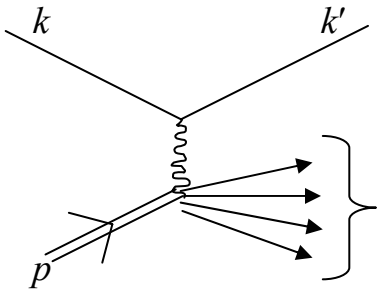

the final state now contains a hadronic system with invariant mass greater than the proton's mass. In other words, additional hadrons are produced other than the initial proton. One can no longer write the hadronic current as

$$J^\mu = \bar{u}(p')[\qquad\qquad]^\mu u(p)$$

since $\bar{u}(p')$ is not the final state.

Instead, one needs to write down a general parameterization of the hadronic tensor:

$$w^{\mu\nu} = -w_1 g^{\mu\nu} + \frac{w_2}{M^2} p^\mu p^\nu + \frac{w_4}{M^2} q^\mu q^\nu + \frac{w_5}{M^2}\left(p^\mu q^\nu + q^\mu p^\nu\right) \qquad (6.29)$$

(Note that the w_3 term, $i\varepsilon^{\mu\nu\alpha\beta} p_\alpha q_\beta \frac{w_3}{2M^2}$, violates parity and is not included here for electromagnetic interaction. It is present for weak interaction.)

Again, the current conservation requires

$$q_\mu w^{\mu\nu} = q_\nu w^{\mu\nu} = 0 \qquad (6.30)$$

Hence, we obtain

$$w_5 = \frac{-p\bullet q}{q^2} w_2 \qquad w_4 = \left(\frac{p\bullet q}{q^2}\right)^2 w_2 + \frac{M^2}{q^2} w_1$$

The hadronic tensor can therefore be expressed as

$$w^{\mu\nu} = w_1\left(-g^{\mu\nu} + \frac{q^\mu q^\nu}{q^2}\right) + \frac{w_2}{M^2}\left(p^\mu - \frac{p\bullet q}{q^2}\right)\left(p^\nu - \frac{p\bullet q}{q^2}q^\nu\right) \qquad (6.31)$$

Unlike the elastic scattering case, where $p\bullet q = -\frac{q^2}{2}$, for inelastic *ep* scattering $p\bullet q \neq -\frac{q^2}{2}$. Also, w_1 and w_2 can be functions of two Lorentz-invariant scalars, rather than just one scalar as in the *ep* elastic scattering case.

Some Lorentz invariant scalars are q^2, $\nu = \frac{p\bullet q}{M}$, $x = \frac{-q^2}{2p\bullet q}$, and $y = \frac{p\bullet q}{p\bullet k} = \frac{E - E'}{E}$.

Also, the invariant mass of the hadronic system is

$$w^2 = \left(p + q\right)^2 = M^2 + 2M\nu + q^2 \qquad (6.32)$$

It can be shown readily that

$$0 \le x \le 1 \quad \text{and} \quad 0 \le y \le 1 \qquad (6.33)$$

For elastic scattering, $x = 1$, $y = 0$.

It is now straight-forward to calculate $L^{\mu\nu}w_{\mu\nu}$, we have (ignoring m)

$$L^{\mu\nu}w_{\mu\nu} = 4w_1\left(k\bullet k'\right) + \frac{2w_2}{M^2}\left[2\left(p\bullet k\right)\left(p\bullet k'\right) - M^2\left(k\bullet k'\right)\right] \qquad (6.34)$$

Note that by parametrizing $w_{\mu\nu}$ directly in the *ep* inelastic scattering, one bypasses the tedious calculation of the traces encountered in the *ep* elastic scattering when J^μ is parameterized (see equations between Equations 6.19 and 6.20).

In the lab frame, noting that, ignoring m_e, we have

$$k\bullet k' = EE' - EE'\cos\theta = 2EE'\sin{}^{\theta}\!/_{2}$$

$$p\bullet k = EM \qquad p\bullet k' = E'M$$

Therefore,

$$L^{\mu\nu}w_{\mu\nu} = 4EE'\left\{\cos^2\frac{\theta}{2}w_2\left(\nu,q^2\right) + \sin^2\frac{\theta}{2}2w_1\left(\nu,q^2\right)\right\} \tag{6.35}$$

and the cross section can be written as

$$\left.\frac{d\sigma}{dE'd\Omega}\right|_{lab} = \frac{\alpha^2}{4E^2\sin^4\theta/2}\left\{w_2\left(\nu,q^2\right)\cos^2\frac{\theta}{2} + 2w_1\left(\nu,q^2\right)\sin^2\frac{\theta}{2}\right\} \tag{6.36}$$

Note that instead of writing the cross section as $\frac{d\sigma}{d\Omega}$, like in the *ep* elastic scattering (Equation 6.20), the inelastic *ep* cross section is also a function of E′.

It is instructive to write the $e^-\mu^- \rightarrow e^-\mu^-$ scattering cross section in a similar form

$$\left.\frac{d\sigma}{dE'd\Omega'}\right|^{lab}_{e^-\mu^-\rightarrow e^-\mu^-} = \frac{\alpha^2}{4E^2\sin^4\theta/2}\left(\cos^2\frac{\theta}{2} - \frac{q^2}{2m^2}\sin^2\frac{\theta}{2}\right)\delta\left(\nu + \frac{q^2}{2m}\right) \tag{6.37}$$

The delta function in Equation 6.37 reflects the fact that $e^-\mu^- \rightarrow e^-\mu^-$ is an elastic scattering.

If proton is a point particle with mass *m*, then a comparison of Equation 6.36 with Equation 6.37 shows that

$$\begin{aligned} w_2\left(\nu,q^2\right) &= \delta\left(\nu + q^2/2m\right) \\ 2w_1\left(\nu,q^2\right) &= -\frac{q^2}{2m^2}\delta\left(\nu + q^2/2m\right) \end{aligned} \tag{6.38}$$

The δ function in Equation 6.38 implies that w_1 and w_2 are functions of one variable only in this case.

One can consider another limiting case for Equation 6.36:

For $e^- p \rightarrow e^- p$ elastic scattering (where p is no longer a point-like particle), the cross section is

$$\left.\frac{d\sigma}{dE' d\Omega}\right|_{lab} = \frac{\alpha^2}{4E^2 \sin^4 \theta/2}\left(\frac{G_E^2 + \tau G_M^2}{1+\tau}\cos^2\frac{\theta}{2} + 2\tau G_M^2 \sin^2\frac{\theta}{2}\right) \delta\left(\nu + q^2/2m\right) \tag{6.39}$$

In the elastic limit of the inelastic $ep \rightarrow e'x$ scattering ($x \rightarrow 1$), the cross section should be the same as in Equation 6.39. Therefore, one obtains

$$\begin{aligned} w_2\left(\nu, q^2\right) &= \frac{G_E^2 + \tau G_M^2}{1+\tau}\delta\left(\nu + \frac{q^2}{2M}\right) \\ 2w_1\left(\nu, q^2\right) &= 2\tau G_M^2 \delta\left(\nu + \frac{q^2}{2M}\right) \end{aligned} \tag{6.40}$$

Equation 6.40 provides useful constraints on w_1 and w_2 at the kinematic limit of $x \rightarrow 1$ (elastic scattering).

The similarity of the $ep \rightarrow e'x$ and $\gamma^* p \rightarrow x$ processes, namely

suggests that there should be a connection between the hadronic tensor $w_{\mu\nu}$ and the photon-proton total cross section. It can be shown that

$$\sigma^{tot}\left(\gamma^* p \rightarrow x\right) = \frac{4\pi^2\alpha}{k}\varepsilon^{\mu^*}\varepsilon^{\nu} w_{\mu\nu} \tag{6.41}$$

where k is the γ^* flux, and ε is the polarization vectors of the virtual photon.

Choosing the *z* axis as the momentum direction of the virtual photon, we can write the polarization vectors as follows:

$$q = \left(\nu, 0, 0, \left(\nu^2 - q^2\right)^{1/2}\right)$$
$$\varepsilon\left(\lambda = \pm 1\right) = \mp\sqrt{\frac{1}{2}}\left(0; 1, \pm i, 0\right) \tag{6.43}$$

for longitudinally polarized virtual photon

The gauge invariance $q \bullet \varepsilon = 0$ is clearly satisfied.

From Equations 6.41 – 6.43, it is straight-forward to show in the lab frame, that

$$w_1\left(\nu, q^2\right) = \frac{K}{4\pi^2\alpha}\sigma_T \qquad \left(\sigma_T = \frac{1}{2}\left(\sigma_+ + \sigma_-\right)\right)$$
$$w_2\left(\nu, q^2\right) = \frac{K}{4\pi^2\alpha}\left(1 - \frac{\nu^2}{q^2}\right)\left(\sigma_T + \sigma_L\right) \tag{6.44}$$

Equation 6.44, together with Equation 6.36, lead to the following expressions connecting the $ep \rightarrow e'x$ inelastic scattering cross section with the photon-proton total cross sections:

$$\left.\frac{d\sigma}{dE' d\Omega}\right|_{lab} = \Gamma\left(\sigma_T + \varepsilon\sigma_L\right) \tag{6.45}$$

where

$$\Gamma = \frac{\alpha K}{2\pi^2\left|q^2\right|}\frac{E'}{E}\frac{1}{1-\varepsilon}$$
$$\varepsilon = \left(1 - 2\frac{\nu^2 - q^2}{q^2}\tan^2\frac{\theta}{2}\right)^{-1} \tag{6.46}$$

3. Parton Model

How do we expect the structure functions w_1 and w_2 to behave? It is instructive to consider some special cases:

1) $ep \rightarrow ep$ elastic scattering from a 'point-like' proton

As shown in Equation 6.38

$$w_2\left(\nu, q^2\right) = \delta\left(\nu + {q^2}/{2m}\right)$$

$$2w_1\left(\nu, q^2\right) = -\frac{q^2}{2m^2}\delta\left(\nu + {q^2}/{2m}\right)$$

Defining $Q^2 = -q^2,\ x = {Q^2}/{2M\nu}$,

and noting that $\delta\left(\nu - {Q^2}/{2m}\right) = \frac{1}{\nu}\delta\left(1 - {Q^2}/{2m\nu}\right)$,

then

$$\begin{aligned} \nu w_2 &= \delta\left(1 - x\right) \\ 2Mw_1 &= x\delta\left(1 - x\right) \end{aligned} \tag{6.47}$$

If one plots νw_2 versus ${Q^2}/{2M\nu}$, then one would observe that νw_2 corresponds to a single line located at ${Q^2}/{2M\nu} = 1$

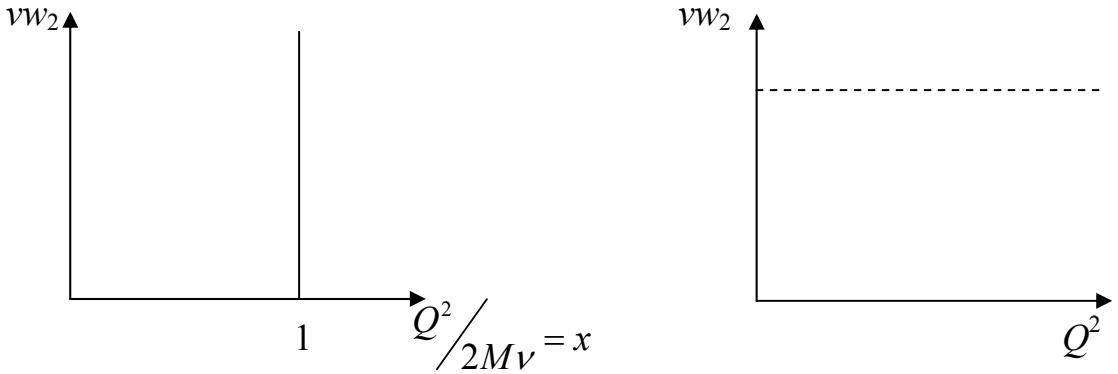

Also, the value of νw_2 would be independent of Q^2.

2) $ep \rightarrow ep$ Elastic Scattering from a Composite Proton

In this case, Equation 6.40 gives

$$w_2\left(\nu,q^2\right)=\frac{G_E^2+\tau G_M^2}{1+\tau}\delta\left(\nu+\frac{q^2}{2M}\right)$$

$$2w_1\left(\nu,q^2\right)=2\tau G_M^2\delta\left(\nu+\frac{q^2}{2M}\right)$$

$$\tau=-\frac{q^2}{4M^2}$$

or

$$\begin{aligned}\nu w_2\left(\nu,q^2\right)&=\frac{G_E^2+\tau G_M^2}{1+\tau}\delta\left(1-\frac{Q^2}{2M\nu}\right)\\ 2Mw_1\left(\nu,q^2\right)&=\frac{Q^2}{2M\nu}G_M^2\delta\left(1-\frac{Q^2}{2M\nu}\right)\end{aligned}\qquad(6.48)$$

νw_2 and $2Mw_1$ are no longer related as in Equation 6.47 (where $2Mw_1 = x\,\nu w_2$). If one plots νw_2 as a function of $Q^2/2M\nu$, one would still observe a single peak at $Q^2/2M\nu = 1$.

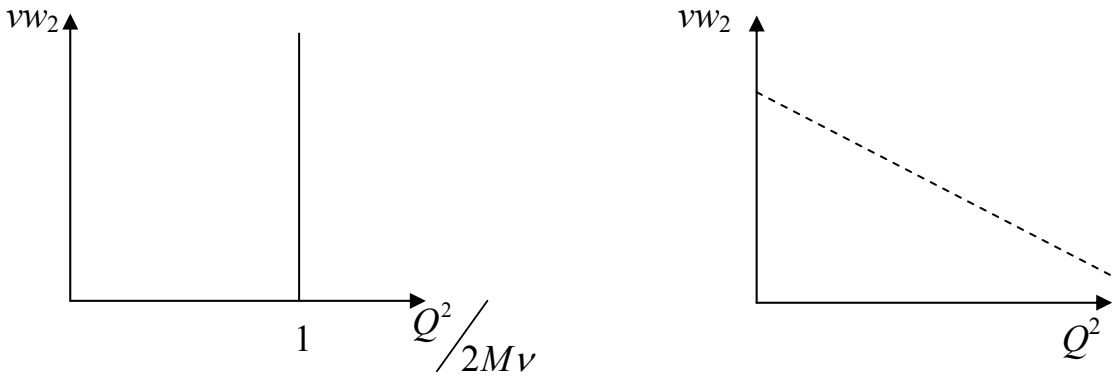

However, νw_2 would drop rapidly versus Q^2 since G_E^2 and G_M^2 both fall off rapidly as a function of Q^2.

Similarly, for $ep \rightarrow eN^*$ inelastic excitation of a nucleon resonance N^*, one also observes a rapid fall-off of νw_2 versus Q^2.

3) $eq \rightarrow eq$ Elastic Scattering

q signifies a point-like particle (quark) which carries a charge e_i and has a mass $m_q = x'M$. The cross section for $eq \rightarrow eq$ elastic scattering is (for spin-½ q)

$$\frac{d\sigma}{dE'd\Omega} = \frac{\alpha^2}{4E^2 \sin^4 \theta/2} e_i^2 \left\{ \cos^2 \frac{\theta}{2} - \frac{q^2}{2m_q^2} \sin^2 \frac{\theta}{2} \right\} \delta\left(\nu + \frac{q^2}{2m_q} \right) \tag{6.49}$$

The structure functions in this case are

$$\begin{aligned} w_2\left(\nu, q^2\right) &= e_i^2 \delta\left(\nu + \frac{q^2}{2m_q} \right) = e_i^2 \frac{1}{\nu} \delta\left(1 - \frac{Q^2}{2M\nu x'} \right) \\ 2w_1\left(\nu, q^2\right) &= e_i^2 \frac{Q^2}{2M^2 \nu x'^2} \delta\left(1 - \frac{Q^2}{2M\nu x'} \right) \end{aligned} \tag{6.50}$$

νw_2 plotted as a function of $Q^2/2M\nu$ would peak at x'

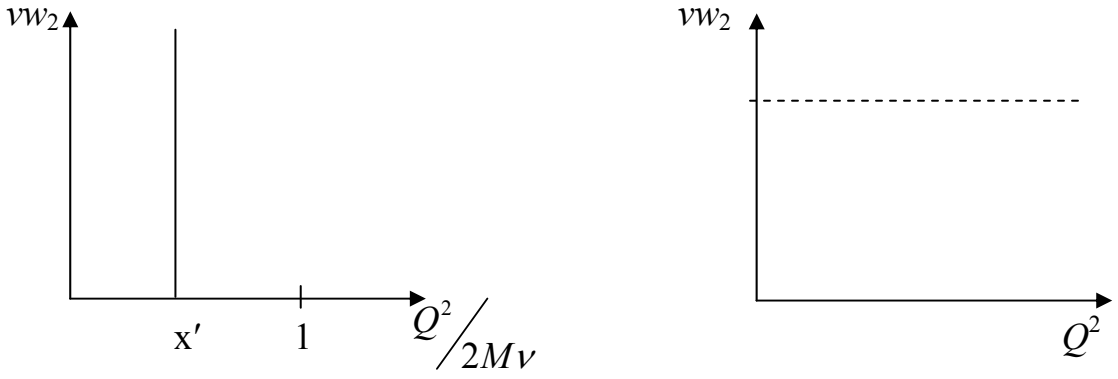

while νw_2 is independent of Q^2.

4) $ep \rightarrow e'x$ where p consists of point-like charged partons

This is a generalization of 3). We define $f_i(x')$ as the probability for parton of type i to have a fraction x' of nucleon's momentum (mass). Equation 6.50 then generalizes to

$$\begin{aligned} \nu w_2\left(\nu, q^2\right) &= \sum_i \int_0^1 dx' f_i\left(x'\right) e_i^2 \delta\left(1 - \frac{Q^2}{2M\nu x'}\right) \\ &= \sum_i e_i^2 \frac{Q^2}{2M\nu} f_i\left(\frac{Q^2}{2M\nu}\right) \end{aligned} \tag{6.51}$$

where we use

$$\delta\left(1 - \frac{Q^2}{2M\nu x'}\right) = \left[\delta\left(x' - \frac{Q^2}{2M\nu}\right)\right] x'$$

Since $\frac{Q^2}{2M\nu}$ is defined as x, Equation 6.51 can also be written as

$$\nu w_2\left(\nu, q^2\right) = \sum_i e_i^2 x f_i\left(x\right) \tag{6.52}$$

Similarly, one can show that

$$M w_1\left(\nu, q^2\right) = \frac{1}{2x} \sum_i e_i^2 x f_i\left(x\right) \tag{6.53}$$

Equations 6.52 and 6.53 show that νw_2 and $M w_1$ exhibit the 'scaling' behavior. Namely, they only depend on a single parameter x. One therefore defines the following structure functions:

$$\begin{aligned} F_2 &= \nu w_2 = \sum_i e_i^2 x f_i\left(x\right) \\ F_1 &= M w_1 = \frac{1}{2x} F_2\left(x\right) \end{aligned} \tag{6.54}$$

The scaling behavior of νw_2 and Mw_1 was observed in the pioneering 'deep-inelastic' scattering experiments. It was called 'deep inelastic' since the invariant mass w of the hadronic system is much larger that the proton mass $w >> M$.

Note that the relation $F_1(x) = F_2(x)/2x$ is a result of the assumption that the parton has spin-½ (Equation 5.49). If one assumes that the partons are spin-0 object, then the relevant scattering cross sections would be the $e^-\pi^- \rightarrow e^-\pi^-$:

$$\frac{d\sigma}{dE'd\Omega'} = \frac{\alpha^2}{4E^2 \sin^4 \theta/2} \cos^2 \frac{\theta}{2} \delta\left(\nu + \frac{q^2}{2m}\right) \tag{6.55}$$

In this case, we have

$$\begin{aligned} w_2 &= \delta\left(\nu + \frac{q^2}{2m}\right) \\ w_1 &= 0 \end{aligned} \tag{6.56}$$

which implies

$$F_1(x) = 0 \tag{6.57}$$

Experiments favor $2x\,F_1(x) = F_2(x)$, rather than $F_1(x) = 0$. Therefore, they support the interpretation that charged partons have spin-½.

Equations 6.44 can also be written as

$$\begin{aligned} \sigma_T &= \left(\frac{4\pi^2\alpha}{K}\right) w_1 = \frac{4\pi^2\alpha}{MK} F_1(x) \\ \sigma_L &= \left(\frac{4\pi^2\alpha}{K}\right)\left[\left(1 + \frac{\nu^2}{Q^2}\right) w_2 - w_1\right] = \left(\frac{4\pi^2\alpha}{K}\right)\left[\left(\frac{1}{\nu} + \frac{1}{2Mx}\right) F_2 - \frac{F_1}{M}\right] \\ &\simeq \left(\frac{4\pi^2\alpha}{K}\right)\left[\frac{1}{2Mx}\left(F_2 - 2xF_1\right)\right] \end{aligned} \tag{6.58}$$

where we use $\frac{1}{\nu} \to 0$ for large ν.

Equation 6.58 shows that for spin-½ parton, $F_2 = 2xF_1$, and $\sigma_L \to 0$. In contrast, for spin-0 parton, Equation 6.58 shows that $\sigma_T = 0$. Hence, we have

$$\begin{aligned} &\frac{\sigma_L}{\sigma_T} \to 0 \quad \text{for spin} - \tfrac{1}{2} \text{ partons} \\ &\frac{\sigma_T}{\sigma_L} \to 0 \quad \text{for spin} - 0 \text{ partons} \end{aligned} \tag{6.59}$$

Equation 6.59 can be readily understood from a consideration of parton's helicity and γ^*'s helicity. In the Breit frame,

spin-½ case:

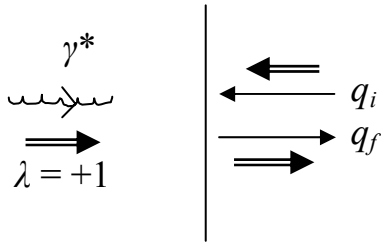

helicity conservation requires $\lambda = +1$
γ^* be absorbed in this case, and
γ^* cannot have $\lambda = 0$. Similarly, $\lambda = -1$
γ^* is required if the q_i is left-handed

spin-0 case:

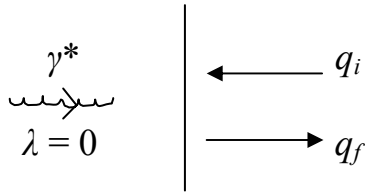

Since a spinless q_i cannot absorb
$\lambda = \pm 1$ γ^*, only $\lambda = 0$ γ^* can contribute.

The phenomenon of scaling was first observed at SLAC in the late 1960's. As the following figure shows, as the beam energy increases the inelastic cross sections rise as w increases. At large w, the underlying process is the $eq \to eq$ elastic scattering.

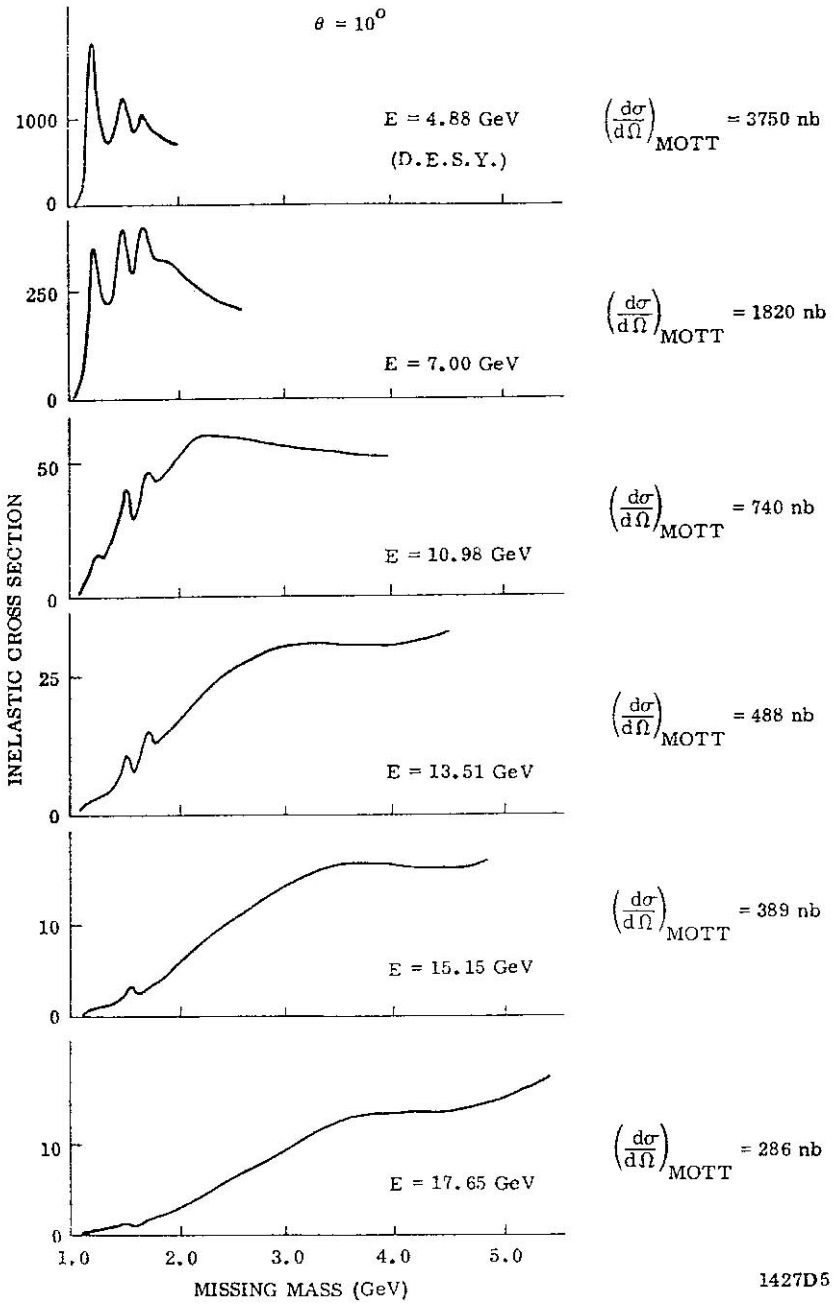

Figure 7. Visual fits to spectra showing the scattering of electrons from hydrogen at 10^{o} for primary energies, *E*, from 4.88 GeV to 17.65 GeV. The elastic peaks have been subtracted and radiative corrections applied. The cross sections are expressed in nanobarns per GeV per steradian.

A similar pattern was also observed when the inelastic cross section was measured at a fixed beam energy, but with the spectrometer angle (scattering angle) varying from very small ($\theta = 1.5^{o}$) to larger ($\theta = 18^{o}$) angles. As the momentum transfer increases, the excitations of the nucleon resonances $\left(N^{*},\ \Delta^{*}\right)$ fall off rapidly. However, the cross sections for deeply inelastic scattering (large w) remain sizeable.

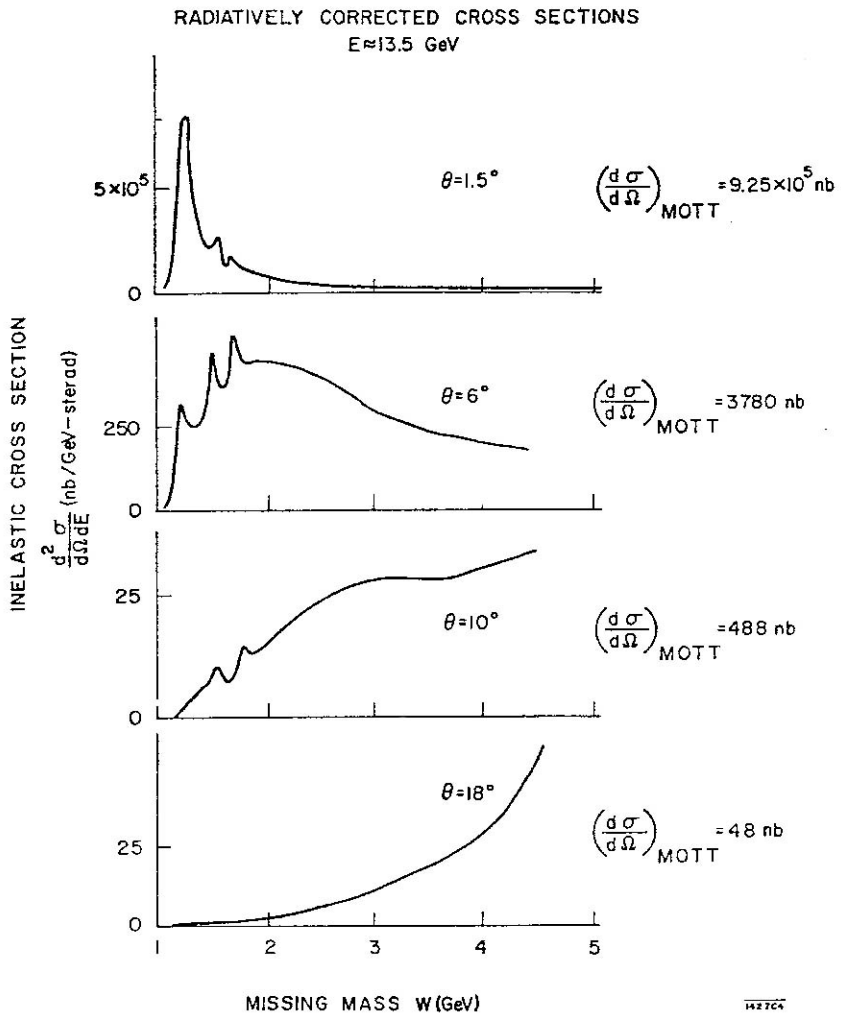

Figure 8. Visual fits to spectra showing the scattering of electrons from hydrogen at a primary energy E of approximately 13.5 GeV, for scattering angles from 1.5^{o} to 18^{o}.

The scaling behavior of νw_2 (= F_2) was observed as shown in the following figure:

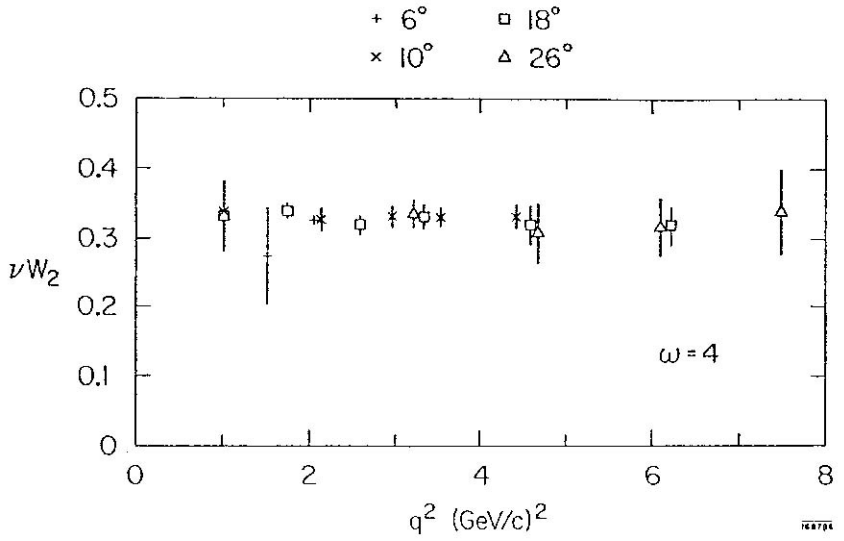

FIGURE 17. νW_2 for the proton as a function of q^2 for $W > 2$ GeV, at $\omega = 4$. Results from (7, 8, and 49).

In this figure, νw_2 is shown to be independent of Q^2 for a fixed value of w $\left(w = 1/x\right)$.

The SLAC data also provided the first direct evidence for the existence of 'sea' quarks. As shown below, $2M_p w_1$, which is $F_1(x)$, was observed to rise as w increases $\left(w = 1/x\right)$. The large parton density at small-x is due to the gluon splitting into quark-antiquark sea.

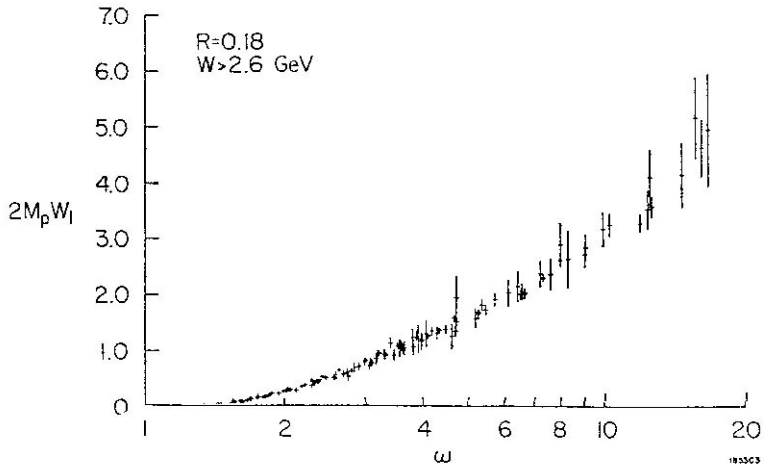

The SLAC experiments have used both the hydrogen and deuterium targets to extract the F_2 structure functions for proton and for neutron. Recall that

$$\begin{aligned} F_2^p / x &= \frac{4}{9}\left(u_p + \bar{u}_p\right) + \frac{1}{9}\left(d_p + \bar{d}_p\right) \quad \text{(ignoring heavier quarks)} \\ F_2^n / x &= \frac{4}{9}\left(u_n + \bar{u}_n\right) + \frac{1}{9}\left(d_n + \bar{d}_n\right) \\ &= \frac{4}{9}\left(d_p + \bar{d}_p\right) + \frac{1}{9}\left(u_p + \bar{u}_p\right) \end{aligned} \tag{6.60}$$

where isospin symmetry is assumed in order to relate the parton distributions in neutron to those in proton.

The ratio, F_2^n / F_2^p, is shown to be close to 1 at $x \to 0$, and it approaches ~ 0.3 as $x \to 1$. Equation 6.60 implies

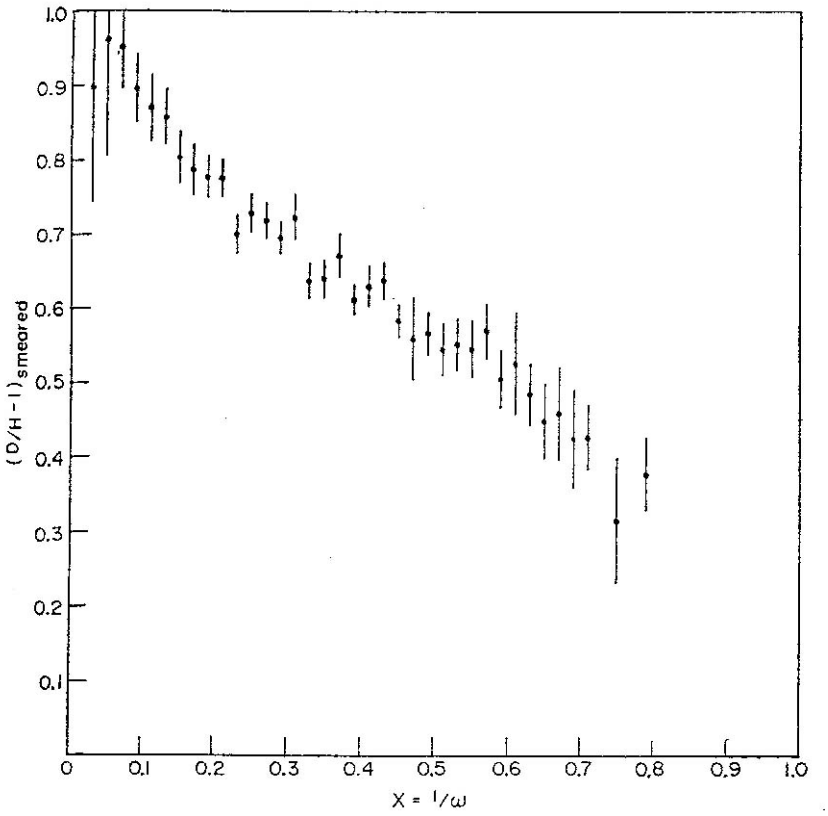

that $\frac{1}{4} \le F_2^n / F_2^p \le 4$, where the ¼ limit is reached when $d_p = 0$, and the limit $F_2^n / F_2^p = 4$ is obtained when $u_p = 0$. The F_2^n / F_2^p data suggests that down quark drops more rapidly than the up quark as $x \to 1$. Indeed, one finds $d(x)/u(x) \simeq (1-x)$ as $x \to 1$.

Another interesting SLAC result is that the $F_2^p - F_2^n$ data can be used to reveal the valence quark distribution. From Equation 6.60, it can be readily shown that

$$F_2^p - F_2^n = \frac{x}{3}\left(u_v(x) - d_v(x)\right) \tag{6.61}$$

where we assume $\bar{u}_p(x) = \bar{d}_p(x)$ and the valence quarks u_v, d_v are defined as

$$\begin{aligned} u_v(x) &= u_p(x) - \bar{u}_p(x) \\ d_v(x) &= d_p(x) - \bar{d}_p(x) \end{aligned} \tag{6.62}$$

The early SLAC data shows that the valence quarks distribution peak at $x \sim ⅓$, as one might expect if the effective quark mass is roughly ⅓ of proton's mass.

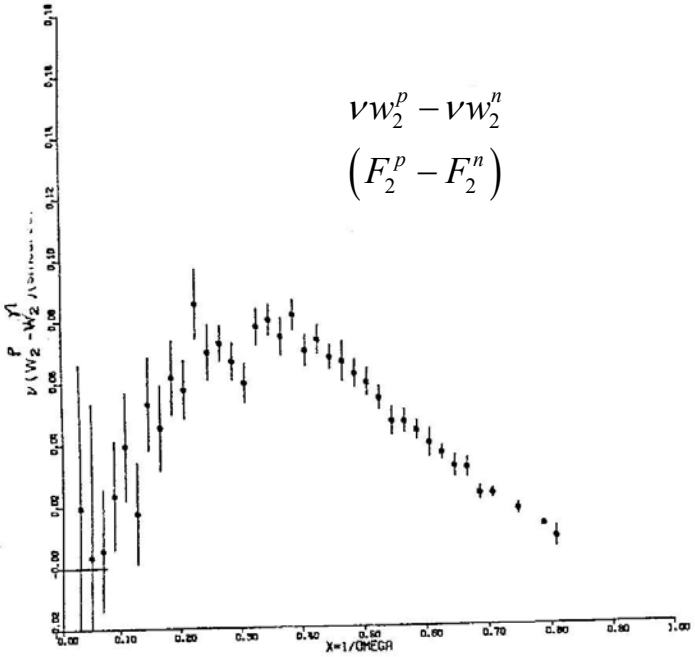

The parton model requires that the total momentum of the nucleon is carried by all partons. In other words,

$$\sum_i \int_0^1 xPf_i(x)\,dx = P$$

hence,

$$\sum_i \int_0^1 xf_i(x)\,dx = 1 \tag{6.63}$$

where P is the momentum of the nucleon, and i signifies various types of partons. Again, important information can be extracted by combining the F_2^p data with the F_2^n data:

$$\int F_2^p(x)\,dx = \frac{4}{9}\int\left(u(x)+\bar{u}(x)\right)x\,dx + \frac{1}{9}\int\left(d(x)+\bar{d}(x)\right)x\,dx \simeq 0.18 \tag{6.64}$$

$$\int F_2^n(x)\,dx = \frac{4}{9}\int\left(d(x)+\bar{d}(x)\right)x\,dx + \frac{1}{9}\int\left(u(x)+\bar{u}(x)\right)x\,dx \simeq 0.12 \tag{6.65}$$

One obtains, from Equation 6.64 and Equation 6.65, the momentum fraction carried by the up and the down quarks.

$$\begin{aligned}\int x\left(u(x)+\bar{u}(x)\right)dx &\simeq 0.36\\ \int x\left(d(x)+\bar{d}(x)\right)dx &\simeq 0.18\end{aligned} \tag{6.66}$$

Therefore, one concludes that the up quarks carry roughly twice the momentum fraction of proton compared with the down quarks. This is consistent with the quark model (assuming sea quarks carry a small fraction of the momentum).

Equation 6.66 also implies that ~ 50% of the proton momentum is carried by neutral partons. Indeed, it is now quite well established that gluons are responsible for ~50% of the nucleon's momentum. The gluon distribution function, $g(x)$, can be determined from processes such as jet production, or from the scaling violation in DIS, which is due to the coupling between quarks and gluons.

The structure function measured in DIS is a sum of quarks and antiquarks with various flavors. It is useful to isolate the quark distribution of a particular flavor. This 'flavor decomposition' can be made by using a variety of techniques:

a) Since F_2^p is mostly sensitive to $u(x)$ while F_2^n is sensitive to $d(x)$, a comparison between F_2^p and F_2^n can provide information on $u(x)$ and $d(x)$.

b) Semi-inclusive DIS

In this type of measurement, a hadron (usually an energetic pion or kaon) is detected in coincidence with the inelastically scattered electron. If the virtual photon struck a $u(d)$ quark, this quark is most likely to hadronize into a $\pi^+(\pi^-)$ meson. Therefore, the 'flavor' of the struck quark can be reasonably well determined.

c) The Drell-Yan Process

The Drell-Yan process is basically an electromagnetic process occurring in hadron-hadron interaction. The underlying mechanism is the annihilation of the quark-antiquark pair into a virtual photon, which

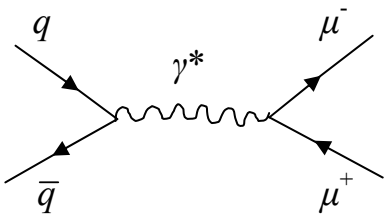

subsequently decays into a pair of charged leptons ($\mu^+\mu^-$, or e^+e^-).

It has been demonstrated that proton-proton and proton-nucleus induced Drell-Yan process is very sensitive to the antiquark distribution in the nucleon and/or nucleus. Furthermore, one can use the Drell-Yan process to measure the quark distributions of mesons. Indeed, the $\pi^{\pm}N \to \mu^+\mu^- x$ and $K^{\pm}N \to \mu^+\mu^- x$, as well as the $\bar{p}N \to \mu^+\mu^- x$ reactions have been measured, and they provide the rare information we have so far on the parton distributions in π, K and $\bar{p}$. Note that these particles cannot be studied in Deep Inelastic Scattering experiments since they are not available as targets.

d) Generalized Drell-Yan Process: *W/Z* production

The Drell-Yan process can be generalized to describe *W/Z* production in hadron-hadron collider. The underlying processes involve a quark-antiquark annihilation into the charge *W* boson or the neutral *Z* boson. By comparing W^+ and W^- production, one can isolate the contributions from *u* versus *d* quarks (and $\overline{u}$ versus $\overline{d}$ too).

e) Neutrino-Induced DIS

As will be explained in the next chapter, neutrino induced DIS reactions are very effective in separating the quark distributions from the antiquark distributions. Of particular interest is the possibility of using semi-inclusive *ν*-induced DIS to determine the strange (and anti-strange) quark distributions in the nuclei. This is accomplished by detecting the $\mu^+\mu^-$ pair from the *ν*-induced DIS.

The mechanism for producing a $\mu^+\mu^-$ pair in *ν*-induced DIS is as follows:

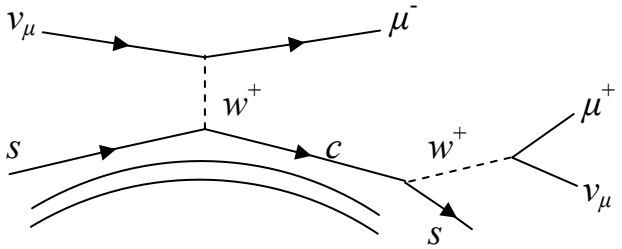

The μ^- is from the (ν_μ, μ^-) process, and the μ^+ is from the charm decay. In a similar fashion, $\overline{\nu}_\mu$ beam can be used to probe the $\overline{s}$ distribution in the nucleon. Although

$\int_0^1 s(x) - \bar{s}(x)\,dx = 0$, it is possible that $s(x)$ and $\bar{s}(x)$ have different dependences on x such that at certain x, $s(x) - \bar{s}(x) \neq 0$.

Symmetries in Parton Distributions

It is useful to use symmetry to connect various parton distributions. Some examples are:

a) Isospin Symmetry

This allows us to make connection between the parton distributions in hadrons which are isospin partners of each other. The proton and neutron form an isospin doublet, and one can use isospin symmetry to relate their parton distributions:

$$u_p(x) = d_n(x) \qquad d_p(x) = u_n(x)$$
$$\bar{u}_p(x) = \bar{d}_n(x) \qquad \bar{d}_p(x) = \bar{u}_n(x)$$

Similarly, π^+ and π^- are members of the isospin triplet, and their parton distributions are related:

$$\begin{aligned} u_{\pi^+}(x) &= d_{\pi^-}(x) & d_{\pi^+}(x) &= u_{\pi^-}(x) \\ \bar{u}_{\pi^+}(x) &= \bar{d}_{\pi^-}(x) & \bar{d}_{\pi^+}(x) &= \bar{u}_{\pi^-}(x) \end{aligned} \tag{6.67}$$

b) Charge-Conjugation Symmetry

For two hadrons which are related by particle-antiparticle operation (charge-conjugation), their parton distributions are also related. For example, the parton distributions in p and $\bar{p}$ are connected:

$$\begin{aligned} u_p(x) &= \bar{u}_{\bar{p}}(x) & d_p(x) &= \bar{d}_{\bar{p}}(x) \\ \bar{u}_p(x) &= u_{\bar{p}}(x) & \bar{d}_p(x) &= d_{\bar{p}}(x) \end{aligned} \tag{6.68}$$

Similarly, π^+ and π^- are related by charge-conjugation operation (they are antiparticles of each other).

Hence,

$$\begin{aligned} u_{\pi^+}(x) &= \bar{u}_{\pi^-}(x) \qquad d_{\pi^+}(x) = \bar{d}_{\pi^-}(x) \\ \bar{u}_{\pi^+}(x) &= u_{\pi^-}(x) \qquad \bar{d}_{\pi^+}(x) = d_{\pi^-}(x) \end{aligned} \tag{6.69}$$

From Equations 6.67 and 6.69, we obtain

$$\begin{aligned} u_{\pi^+}(x) = \bar{d}_{\pi^+}(x) = d_{\pi^-}(x) = \bar{u}_{\pi^-}(x) = v_\pi(x) \\ \bar{u}_{\pi^+}(x) = d_{\pi^+}(x) = u_{\pi^-}(x) = \bar{d}_{\pi^-}(x) = s_\pi(x) \end{aligned} \tag{6.70}$$

We conclude that there are only two parton distributions, $v_\pi(x)$ and $s_\pi(x)$, the valence and sea quark distributions, required to describe π^+ and π^-.

c) SU(3) Symmetry

The SU(3) symmetry can be used to relate the parton distributions of various SU(3) multiplets. For example, the $\Sigma^+(uus)$ parton distributions are related to proton (uud)'s distributions as follows

$$\begin{aligned} u_p(x) &= u_{\Sigma^+}(x) \\ s_{\Sigma^+}(x) &= d_p(x) \\ s_p(x) &= d_{\Sigma^+}(x) \end{aligned} \tag{6.71}$$

Since the SU(3) symmetry is known to be broken, Equation 6.71 is only approximately true. Experimentally, the parton distributions of the hyperon (like Σ^+) can be measured using the Drell-Yan process with a hyperon beam. However, in practice, these are difficult measurements and have not been done yet.

Spin-Dependent Structure Functions

Polarized DIS using polarized electron or muon beams scattering off polarized hydrogen or deuterium targets has been used to determine the spin-dependent structure functions $g_1(x)$ and $g_2(x)$. This is an active area of research. From all experiments carried out so far, it was found that only 30% of proton's spin is carried by the up and down quarks. The other 70% must reside in sea quarks,

gluons, or/and orbital angular momentum. However, it is not yet clear how proton's spin is distributed into these various components.